J Mater Sci: Mater Electron (2015) 26:1239–1245
DOI 10.1007/s10854-014-2532-8

# Investigation, characterization and effect of substrate position on thick AlN layers grown by high temperature chemical vapor deposition

**Dian Zhang · Fa-Min Liu · Lu-Gang Cai**

Received: 10 September 2014 / Accepted: 17 November 2014 / Published online: 26 November 2014
© Springer Science+Business Media New York 2014

**Abstract** Thick AlN layers are grown on c-sapphire at 1,300 °C in turbulent, laminar and 45° oblique laminar injection respectively by a homebuilt hot-wall high temperature chemical vapor deposition system (HTCVD) and characterized by SEM, XRD, Raman and optical absorption spectra. The results demonstrate that high quality and 20 μm thick (002) AlN epilayer with full width at half maximum of 1,010 arcsec is grown in 45° oblique laminar injection at growth rate of 24 μm/h, while 28 μm thick (002) AlN epilayer and 46 μm thick (002)-oriented columnar AlN layer with rough surface and larger misorientation are grown in laminar and turbulent injection at growth rate of 34 and 55 μm/h respectively. Meanwhile, the epilayer grown in 45° oblique laminar injection exhibits sharper absorption edge and larger optical band gap of 5.93 eV than that of other two layers. Furthermore, the proposed model suggests that column growth mode governs the growth in turbulent injection with high source concentrations, resulting in (002)-oriented columnar layer with large misorientation. In contrast, Stranski–Krastanov mode governs the growth in laminar injection and 45° oblique laminar injection with decreased source concentrations, leading to nonuniform and uniform (002) epilayer, respectively. Therefore, the HTCVD with 45° oblique laminar injection can be used to grow high quality thick (002) AlN epilayer at high growth rate and low cost.

D. Zhang · F.-M. Liu (✉) · L.-G. Cai
Department of Physics, School of Physics and Nuclear Energy Engineering, Beihang University, Beijing 100191, China
e-mail: fmliu@buaa.edu.cn

## 1 Introduction

The III-nitride semiconductors show growing importance in high-power and high-frequency electron device as well as optoelectronic device today. With the wide application of GaN-base photoelectric devices, increasingly interests have been focused on AlN due to its widest direct bandgap in III-nitrides and close-matched lattice with GaN [1–4]. AlN epilayer prepared by metal organic chemical vapor deposition (MOCVD) [5] and molecular beam epitaxy (MBE) [6] can be used as heteroepitaxial template. AlN bulk single crystal is grown by sublimation [7–9] and solution methods [10, 11] in order to obtain native AlN wafer. Hydride vapor phase epitaxy (HVPE) [12–14] can be applied to prepare free-standing AlN wafer as well. However, these methods are expensive in respect of their equipment and source material, introducing obstacles to massive production and broad application of AlN wafer.

In comparison with all above-mentioned methods, chemical vapor deposition (CVD) can produce thick AlN layer at relative high growth rate and very low cost with simple system which are suitable for massive production. However, the conventional CVD usually produce AlN polycrystalline layer rather than epilayer [15–17] perhaps due to inappropriate parameter, such as low growth temperature which is limited by quartz reactor or improper substrate position which is closely related to the gas injection mode in the reactor. Recently, we develop an alumina hot-wall high temperature chemical vapor deposition system (HTCVD), in which AlN epilayers are grown successfully in temperature range of 1,100–1,500 °C [18]. However, the effects of substrate position and gas injection mode on the growth of AlN layers at high temperature remain unclear. In this study, we grow thick AlN layers in three different gas injection modes which varied with substrate positions in the

reactor respectively. The results demonstrate that the structure and property of the thick AlN layer depends strongly on gas injection mode. Thick AlN epilayer with high quality can be grown in 45° oblique laminar injection, indicating that the developed HTCVD is an inexpensive alternative to prepare thick AlN epilayer and free-standing AlN wafer.

## 2 Experimental

### 2.1 Growth procedure

The main technique features and growth procedure of the HTCVD are reported in detail previously [18]. Solid anhydrous $AlCl_3$ (Analytical reagent 99 %) and $NH_3$ (5 N) are used as sources, and Ar (5 N) is used as carrier and ambient. In this study, three growth runs are conducted in different gas injection modes, i.e. turbulent injection, laminar injection and 45° oblique laminar injection, and the corresponding thick AlN layers are denoted by A, B and C respectively in Fig. 1. In turbulent injection, the substrate is adjacent to $AlCl_3$ nozzle without spacing, while there is a spacing of 15 mm between the substrate and $AlCl_3$ nozzle in laminar injection and 45° oblique laminar injection with 45° tilting angle of substrate relative to horizon. Therefore, the flow fields around the substrate surface are different for layer A, B, and C respectively. All the samples are grown without rotation at 1,300 °C in atmospheric pressure for 50 min, during which the flow rate of $NH_3$, ambient Ar and carrier Ar are all fixed at 1,000 sccm while the flow rate of $AlCl_3$ vapor is 50 sccm. Finally, the HTCVD cools down to room temperature naturally in 50 sccm $NH_3$ and ambient Ar.

### 2.2 Characterization

The morphologies of the layers are studied via a FEG XL s 30 scanning electron microscope (SEM), whose affiliated energy dispersive x-ray (EDX) spectrometer is used to collect EDX spectrum of the layers. The crystal structures are analyzed by X'Pert PRO$^{TM}$ four-circle triple-axis diffractometer using Cu K α line ($\lambda = 0.154059$ nm). The θ–2θ scan is conducted in a 2θ range from 20° to 90° as well as the ω scan mode is conducted at (002) plane of the AlN layer. Micro-Raman scattering is conducted on the layer surface at room temperature in backscattering geometry and $z(xx)\underline{z}$ configuration by 532 nm line of frequency-doubled Nd:YAG laser focusing on a 1 μm spot. The transmittance spectrum is measured in the range from 190 to 900 nm with 1 mm light spot size of deuterium lamp and Xenon lamp in Persee TU-1901.

## 3 Results and discussion

### 3.1 Morphology

Layer A grown in turbulent injection has smooth surface as shown in Fig. 2a. Interestingly, the layer is composed of uniform triangular domains with long crossed boundaries which align in parallel. The typical width of the triangular domains is about 10 μm. Curiously, the enlarged view (Fig. 2b) exhibits swirls of ultrafine grooves throughout the layer surface. These features are different from those typical features of (002) AlN epilayer. Since intensive turbulent flows with high concentrations of the source gases are mixed forcedly and close to the substrate surface, fast growth could "freeze" those eddies within the turbulent flow, resulting in the "swirls" throughout the layer surface. The cross section of the layer in Fig. 2c shows the domain boundaries with spacing of about 10 μm and regular cleavage within the domain, indicating the columnar structure of the layer. According to the thickness of 46 μm and growth duration of 50 min, the growth rate is about 55 μm/h.

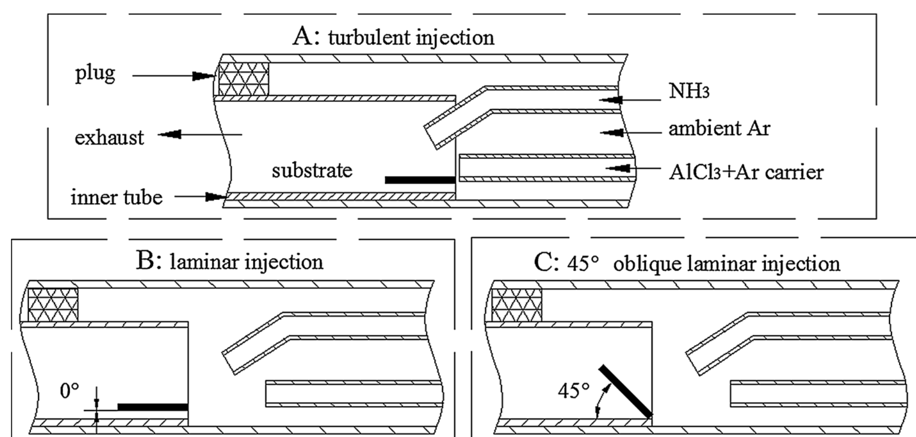


**Fig. 1** The homebuilt alumina hot-wall high temperature chemical vapor deposition, in which the gas injection mode is turbulent injection. **a** Laminar injection, **b** and 45° oblique laminar injection, **c** varied with substrate positions, respectively

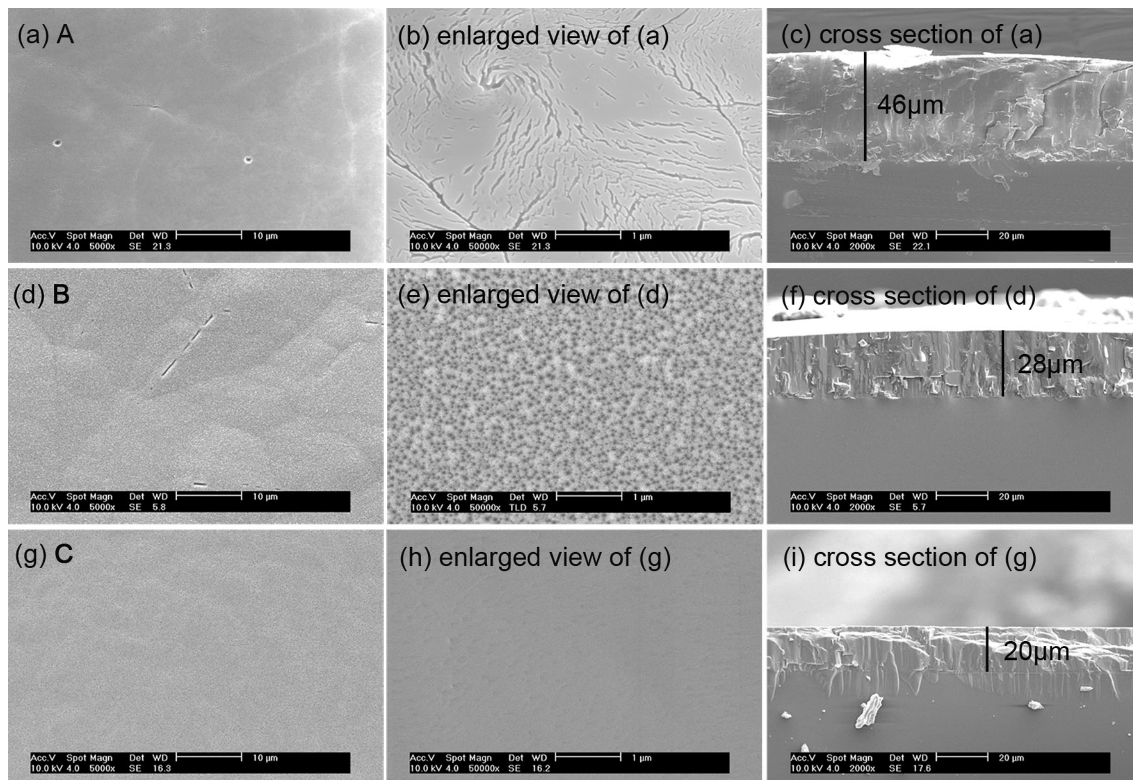


**Fig. 2** Morphologies of the thick AlN layers. **a** Flat surface with large triangle domains of layer *A*; **b** enlarged view of the epilayer surface in (**a**); **c** cross section of layer *A* in (**a**); **d** hillocks at the surface of epilayer *B*; **e** enlarged view of the epilayer surface in (**d**); **f** cross section of epilayer *B* in (**d**); **g** smooth surface of epilayer *C*; **h** enlarged view of the epilayer surface in (**g**); **i** cross section of epilayer *C* in (**g**)

As shown in Fig. 2d, layer B grown in laminar injection has many large hillocks at its surface, indicating mosaic structure and epitaxial growth of AlN layer [19]. The trenches at the layer surface arise from coalescence of neighbored mosaic domains. The nanopits at the layer surface in Fig. 2e originate from coalescence of massive nano islands, indicating that layer B is grown under Stranski–Krastanov (SK) growth mode [20, 21]. The cross section of layer B (Fig. 2f) also shows the regular cleavages. All above features are of typical surface morphologies of (002) AlN epilayer. Compared with layer A, the structure improvement of layer B is owed to laminar flow which dominates the flow pattern when the turbulent flow weakens along the flow direction after the source gases are mixed uniformly. According to its thickness of 28 μm, the growth rate of the layer is about 34 μm/h, which is lower than that of layer A because of the sources dilution caused by diffusion and parasitic reaction during their transportation to the substrate.

Although thick AlN layer is grown in turbulent and laminar injection, its smoothness and uniformity are unsatisfactory. As revealed by Fig. 2c and f, the thickness of layer A and layer B decreases along the flow direction because of source depletion upstream, in accordance with the mass diffusion limited reaction mechanism [14, 22–24]. A solution for the nonuniformity is application of tilting substrate relative to horizon, as been applied in 45° oblique laminar injection (Fig. 1). In comparison with layer B, layer C exhibits very flat surface without hillocks, as shown in Fig. 2g. The enlarged view in Fig. 2h shows that the surface is extremely smooth without visible nanopits and nano islands. The cross section in Fig. 2i shows that its thickness is very uniform and the regular cleavages indicate its high crystal quality. The good uniformity and quality of the layer are owed to further improvement of gas flow pattern and more uniform distribution of the sources in 45° oblique laminar injection. According to the thickness of 20 μm, the growth rate of layer C is about 24 μm/h.

## 3.2 Structure and optical property

The thick AlN layers are characterized by XRD under θ–2θ scan and ω-scan at (002) plane to determine their structures and evaluate their quality respectively. As we know, the θ–2θ scan pattern of (002) AlN epilayer on c-sapphire displays an overlapping pattern of AlN (002), AlN (004) and sapphire (006). Accordingly, layer C is typical (002) AlN epilayer, as revealed by Fig. 3a. In contrast, the pattern of

the layer B has another weak unexpected peak of AlN (110), indicating that there is misorientation to some extent in basal plane of epilayer B. Particularly, the weakened expected peak of AlN (002) together with the intensive and broad unexpected peak of AlN (110) in the pattern of layer A demonstrate that large out-of-plane and in-plane misorientation together with highly preferred expansion of (110) in basal plane take place, resulting in (002)-oriented triangular columnar domains and polycrystalline feature of layer A. In combination with the surface morphology of layer A, we suppose that it is the intensive turbulent flow with high source concentrations which induces fast column growth and leads to the large misorientation of layer A. Since layer A is column structured and less attractive, only epilayer B and epilayer C are characterized by ω-scan at (002) plane to compare their crystal quality. As shown in Fig. 3b, the full width at half maximum (FWHM) of (002) reflection of epilayer B and C are 1,650 and 1,010 arcsec respectively, indicating that the crystal quality of the epilayer C improves remarkably. The improvement could be explained by the conclusion that uniform layer thickness leads to reduction of the tilt and height difference between neighbor mosaics during coalescence so that the dislocations are suppressed [25].

For further investigation on the structure and optical property evolution of the thick layers, Raman scattering and optical absorption of the layers are measured respectively. As seen in Fig. 4a, the Raman scattering of epilayer C exhibit an overlapping spectrum of $E_2$ (low), $E_2$ (high), $A_1$ (LO) modes of AlN and c-sapphire modes, which is the typical feature of the (002) AlN epilayer on c-sapphire according to the selection rules [26]. The weak phonon mode of $E_1$ (TO) indicates misorientation in epilayer B. In contrast, all Raman-active modes of AlN [27] appear in spectrum of layer A, demonstrating large misorintation and polycrystalline component in the layer, in accord with the columnar structure. On the other hand, the optical absorption spectra of the thick layers are different, as shown in Fig. 4b. Epilayer C is more transparent than others two layers and its absorption coefficient α is $<160\ cm^{-1}$ below 5.6 eV (220 nm) according to its thickness $d = 20\ \mu m$ and $\alpha d = $ Absorbance [28, 29]. Moreover, one can realize that the absorbance of layer A and epilayer B increases remarkably with the energy of incident light in comparison with that of epilayer C. The increasing absorbance is attributed to light scattering by the rough surface, domain boundary and misorientation of layer A and epilayer B. Furthermore, we can develop optical band gap energy of the layer through its absorption spectrum by extrapolating the linear part of the absorption edge to energy axis according to Tauc equation $(\alpha h\nu)^2 = B(h\nu - Eg)$ [30, 31]. As revealed by the inset of Fig. 4b, the optical band gap of layer A, B and C are 5.74, 5.86 and 5.93 eV respectively. Some possible causes could be responsible for the variation of the optical band gap energy derived from absorption spectrum. In this study, the decreasing of optical band gap of epilayer B and layer A is mainly attributed to enhancing of light scattering [32, 33], which flattens the optical absorption edge and leads to shrinkage of optical band gap energy.

### 3.3 Gas injection related to growth mode

The morphologies, structures and optical properties of thick AlN layers vary with gas injection modes. Layer A grown in turbulent injection is AlN (002)-oriented columnar layer with large misorientation, layer B grown in laminar injection is AlN (002) epilayer and layer C grown in 45° oblique laminar injection is high quality (002) AlN epilayer respectively. The change of growth mode of the layer is the underlying cause for its structure evolution with gas injection mode. For epilayer B and epilayer C, their

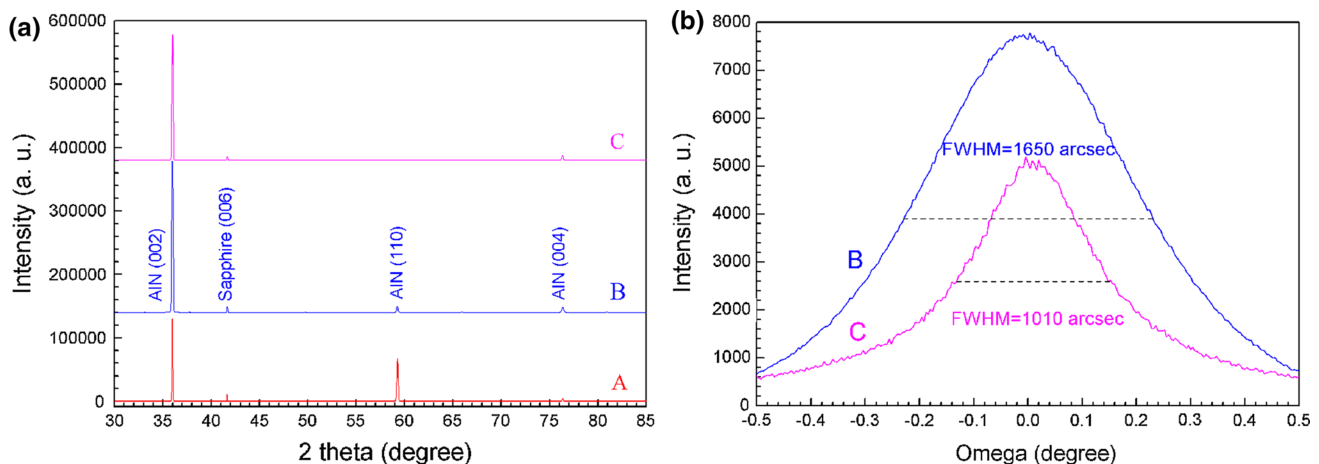


**Fig. 3** XRD patterns of the thick AlN layers. **a** θ–2θ scan; **b** ω-scan

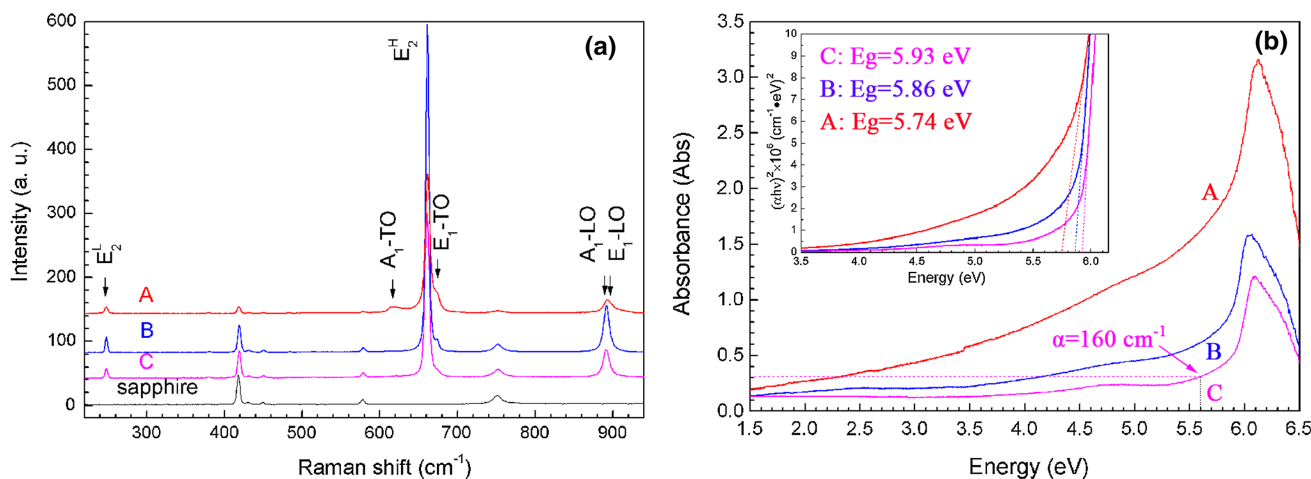


**Fig. 4** Raman scattering and optical property of the thick AlN layers. **a** Raman scattering; **b** optical absorption and optical band gap

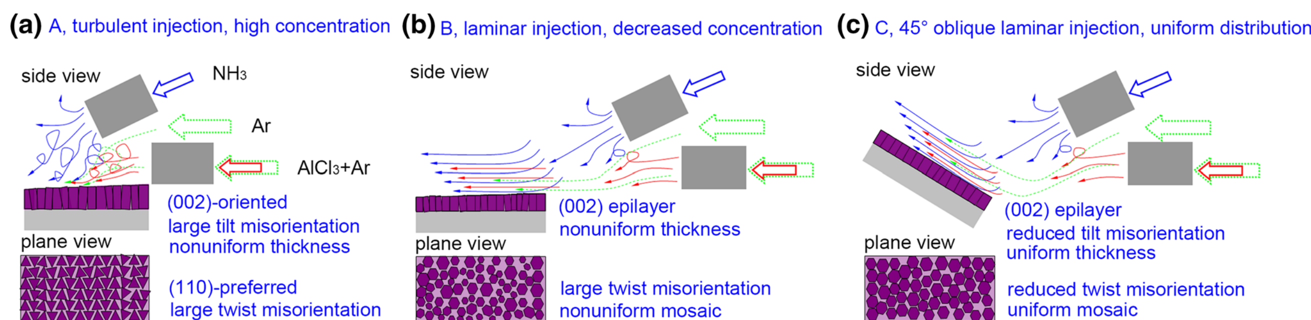


**Fig. 5** Gas injection and growth modes of the thick AlN layers. **a** Turbulent injection and column growth of layer *A*; **b** laminar injection and epilayer *B*; **c** 45° oblique laminar injection and epilayer *C*

growth is in accord with the SK growth mode [20, 21] while the growth mode of layer A agrees with column growth mode. Actually, at the initial growth stage of the heteroepitaxy system for all the three thick AlN layers, pseudomorphic growth takes place under Frank–van der Merwe (FV) mode below critical layer thickness, building nonuniform strain field in the layer due to significant lattice mismatch between AlN layer and sapphire substrate. Subsequently, 3D islands form throughout the surface to reduce the strain energy in the epilayer [21], inducing initial Volmer–Webber (VW) growth.

However, the following growth mode and the final structure of the layer depend on the corresponding gas injection mode. In turbulent injection as depicted in Fig. 5a, high concentrations of $NH_3$ and $AlCl_3$ are injected directly toward the layer surface, leading to high concentration and supersaturation of the source locally. Therefore, high mosaicity derives from large number of surface nuclei and forces the following growth into 3D mode after the initial VW growth, inducing column growth mode [1] and finally resulting in AlN (002)-oriented layer. Furthermore, the forced convection mixing of the sources near the substrate surface, the abrupt expansion of the sources around their nozzles, large local gradient of source concentration and pressure inspire intensive turbulent flow [23], which could even take place in boundary layer of the flow around the AlN layer surface. On one hand, high growth rate leads to large out-of-plane misorientation of the columnar domains and evolution of eddies within the turbulent flow into swirls at layer surface. One the other hand, the turbulent flow could accelerate the diffusion of the reactants which could result in preferred expansion of (110) plane and large in-plane misorientation of the columnar domains. Consequently, the large misorientation weakens (002) peak in the XRD pattern and induces the broad unexpected (110) peak, which is enhanced by preferred expansion of (110) plane of the column domains.

In laminar injection as depicted in Fig. 5b, the source flow becomes uniform and the turbulent flow weakens after mixing and transportation. When the mixture of sources reaches the substrate, the flow pattern turns into laminar flow with decreased concentrations and lower supersaturation due to dilution, diffusion and depletion upstream. Accordingly, layer B is grown at lower growth rate in

steady flow field. Therefore, after the initial VW growth, the growth mode of layer B turns into SK mode of epitaxial growth instead of column growth mode of layer A, finally resulting in AlN (002) epilayer B. However, the weak (110) peak in XRD pattern of the layer indicates that there is discernible misorientation among mosaic domains without highly preferred expansion in basal plane.

The thickness of layer always decreases along the flow direction because of sources depletion upstream in mass transport limited reaction, as revealed by columnar layer A and epilayer B. However, the thickness decrease can be offset and uniform thickness can be obtained by tilting the substrate [24], as revealed by epilayer C grown in 45° oblique laminar injection. Figure 5c demonstrates that 45° oblique laminar injection can distribute the source gases uniformly [23] across the substrate. Meanwhile, the tilting can enhance the projection of downstream substrate into boundary layer [1] and increase the flow velocity due the flow constriction downward so that the Reynolds number goes up and boundary layer decreases, resulting in more uniform growth rate [24]. The uniformity happens not only to the thickness but also to the domain expansion in basal plane of epilayer C, suppressing the misorientation and leading to vanishing of AlN (110) peak in θ–2θ scan and decreased FWHM of the (002) reflection in ω scan of XRD patterns. Therefore, high quality AlN (002) epilayer can be grown in 45° oblique laminar injection.

## 4 Conclusions

In this paper, thick AlN layers are grown on c-sapphire substrates at 1,300 °C in turbulent injection, laminar injection and 45° oblique laminar injection respectively in the developed HTCVD. The characterization of the layers demonstrates that turbulent injection grows AlN (002)-oriented columnar layer with thickness of 46 μm at growth rate of 55 μm/h while laminar injection grows AlN (002) epilayer with thickness of 28 μm at growth rate of 34 μm/h. In contrast, 45° oblique laminar injection grows uniform and high quality AlN (002) epilayer with (002) FWHM of 1,010 arcsec and thickness of 20 μm and at growth rate of 24 μm/h. Moreover, XRD and Raman scattering exhibit that large out-of-plane and in-plane misorientation exists in the layers grown in turbulent and laminar injection while the misorientation is reduced greatly in 45° oblique laminar injection. Meanwhile, the optical absorption spectra show that the epilayer grown in 45° oblique laminar injection has sharper optical absorption edge and larger optical band gap of 5.93 eV than that of other two layers whose rough surface and large misorientation flatten their absorption edge and result in reduced optical band gap of 5.74 and 5.86 eV respectively. Furthermore, the proposed model suggests that column growth governs the growth in turbulent injection with high source concentrations, resulting in AlN (002)-oriented columnar layer and (110)-preferred expansion of columnar domains in basal plane with large out-of-plane and in-plane misorientation. However, SK mode governs the growth in laminar injection and 45° oblique laminar injection with decreased source concentrations and uniform source distribution, resulting in AlN (002) epilayer and high quality AlN (002) epilayer with uniform growth and reduced misorientation, respectively. Therefore, the HTCVD with 45° oblique laminar injection can be used to grow high quality thick (002) AlN epilayer at high growth rate and very low cost.

## References

1. O. Ambacher, J. Phys. D Appl. Phys. **31**, 2653 (1998)
2. P. Ruterana, M. Albrech, J. Neugebauer, *Nitride Semiconductors: Handbook on Materials and Devices* (Wiley-VCH Verlag GmbH & Co. KGaA, Weinheim, 2003), pp. 4–5
3. S.K. O'Leary, B.E. Foutz, M.S. Shur, L.F. Eastman, J. Mater. Sci. Mater. Electron. **17**, 87 (2006)
4. R.T. Bondokov, S.G. Mueller, K.E. Morgan, G.A. Slack, S. Schujman, M.C. Wood, J.A. Smart, L.J. Schowalter, J. Cryst. Growth **310**, 4020 (2008)
5. X.H. Chen, S.P. Li, J.Y. Kang, J. Mater. Sci. Mater. Electron. **19**, S215 (2008)
6. V.N. Jmerik, A.M. Mizerov, D.V. Nechaev, P.A. Aseev, A.A. Sitnikova, S.I. Troshkov, P.S. Kop'ev, S.V. Ivanov, J. Cryst. Growth **354**, 188 (2012)
7. M. Beshkova, Z. Zakhariev, J. Birch, A. Kakanakova, R. Yakimova, J. Mater. Sci. Mater. Electron. **14**, 767 (2003)
8. S.B. Zuo, J. Wang, X.L. Chen, S.F. Jin, L.B. Jiang, H.Q. Bao, L.W. Guo, W. Sun, W.J. Wang, Cryst. Res. Technol. **47**, 139 (2012)
9. R.R. Sumathi, P. Gille, J. Mater. Sci. Mater. Electron. **25**, 3733 (2014)
10. H. Matsubara, K. Mizuno, Y. Takeuchi, S. Harada, Y. Kitou, E. Okuno, T. Ujihara, Jpn. J. Appl. Phys. **52**, 08JE171 (2013)
11. M. Yonenura, K. Kamei, S. Munetoh, J. Mater. Sci. Mater. Electron. **16**, 197 (2005)
12. A. Volkova, V. Ivantsov, L. Leung, J. Cryst. Growth **314**, 113 (2011)
13. T. Nagashima, A. Hakomori, T. Shimoda, K. Hironaka, J. Cryst. Growth **350**, 75 (2012)
14. Y. Katagiri, S. Kishino, K. Okuura, H. Miyake, K. Hiramatu, J. Cryst. Growth **311**, 2831 (2009)
15. T. Goto, J. Tsuneyoshi, K. Kaya, T. Hirai, J. Mater. Sci. **27**, 247 (1992)
16. A. Dollet, Y. Casaux, G. Chaix, C. Dupuy, Thin Solid Film. **406**, 1 (2002)
17. R. Boichot, A. Claude, N. Baccar, A. Milet, E. Blanquet, M. Pons, Surf. Coat. Technol. **205**, 1294 (2010)
18. D. Zhang, F.M. Liu, Y. Yao, X.A. Yang, J. Mater. Sci. Mater. Electron. **25**, 2210 (2014)
19. A. Claudel, E. Blanquet, D. Chaussende, M. Audier, D. Pique, M. Pons, J. Cryst. Growth **311**, 3371 (2009)
20. H.M. Ng, D. Doppalapudi, E. Iliopoulos, T.D. Moustakas, Appl. Phys. Lett. **74**, 1036 (1999)
21. A. Baskaran, P. Smereka, J. Appl. Phys. **111**, 044321 (2012)

22. H. Komiyama, Y. Shimogaki, Y. Egashira, Chem. Eng. Sci. **54**, 1941 (1999)
23. Y.D. Xu, X.T. Yan, *Chemical Vapour Deposition: An Integrated Engineering Design for Advanced Materials* (Springer, London, 2010), pp. 73–162
24. H.O. Pierson, *Handbook of Chemical Vapor Deposition: Principles, Technology and Applications* (Noyes Publications/New York, William Andrew Publishing, New Jersey, 1999), pp. 54–55
25. A. Volkova, V. Ivantsov, L. Leung, J. Cryst. Growth **314**, 113 (2011)
26. J. Senawiratne, Structural and Optical Characterization of Group III-Nitride Compound Semiconductors. Ph.D. dissertation, Georgia State University, Atlanta, Georgia (2006)
27. G. Dhanaraj, K. Byrappa, V. Prasad, M. Dudley, *Handbook of Crystal growth* (Springer, Berlin, 2010), pp. 835–838
28. M. Bickermann, B.M. Epelbaum, O. Filip, P. Heimann, M. Feneberg, S. Nagata, A. Winnacker, Phys. Status Solidi C **7**, 1743 (2010)
29. N.M. Ahmed, Z. Sauli, U. Hashim, Y. Al-Douri, Int. J. Nanoelectron. Mater. **2**, 189 (2009)
30. M. Bickermann, B.M. Epelbaum, O. Filip, P. Heimann, S. Nagata, A. Winnacker, Phys. Status Solidi B **246**, 1181 (2009)
31. S.X. Lu, Y.H. Tong, Y.C. Liu, C.S. Xu, Y.M. Lu, J.Y. Zhang, D.Z. Shen, X.W. Fan, J. Phys. Chem. Sol. **66**, 1609 (2005)
32. D. Barlett, C.A. Ii Taylor, B.D. Wissman, Real-time temperature, optical band gap, film thickness, and surface roughness measurement for thin films applied to transparent substrates, US patent 2013/0321805 A1
33. H.Y. Joo, H.J. Kim, S.J. Kim, S.Y. Kim, J. Vac. Sci. Technol. A **17**, 862 (1999)